I&EC research
Industrial & Engineering Chemistry Research

pubs.acs.org/IECR

Article

Ionic Liquid Selection for the Separation of Refrigerant Mixtures Using Extractive Distillation

Ethan A. Finberg, Max Cordry, Tessie L. May, Kalin R. Baca, and Mark B. Shiflett*

Cite This: *Ind. Eng. Chem. Res.* 2023, 62, 16070−16080

Read Online

ACCESS | Metrics & More | Article Recommendations | Supporting Information

ABSTRACT: Separating azeotropic refrigerant mixtures is needed in the refrigerant industry to prevent the incineration or venting of end-of-life refrigerants. One promising technology for separating the refrigerant mixtures is extractive distillation with ionic liquid as the entrainer. As a continuation of previous work, two refrigerant mixtures are investigated, HFC-125/HFC-143a and HFC-32/HCFC-22, as well as R-449A (an equimass mixture of HFC-32, HFC-125, HFC-134a, and HFO-1234yf), to represent a hydrofluorocarbon/hydrofluoroolefin (HFC/HFO) system. The ionic liquids are selected based on the solubility ratio between the mixture components at elevated pressures (0.5 MPa). The ionic liquid $[P_{(14)666}][TMPP]$ is selected for separating HFC-125/HFC-143a, $[C_2C_1im][TFES]$ is selected for separating HFC-32/HCFC-22, and $[C_2C_1im][SCN]$ is selected for separating HFC-32/HFC-125/HFC-134a/HFO-1234yf. Aspen Plus simulations are completed for systems HFC-125/HFC-143a and HFC-32/HCFC-22, showing that these azeotropic refrigerant mixtures can be separated up to refrigerant purities of 99.5 wt % using the proper ionic liquid entrainers.

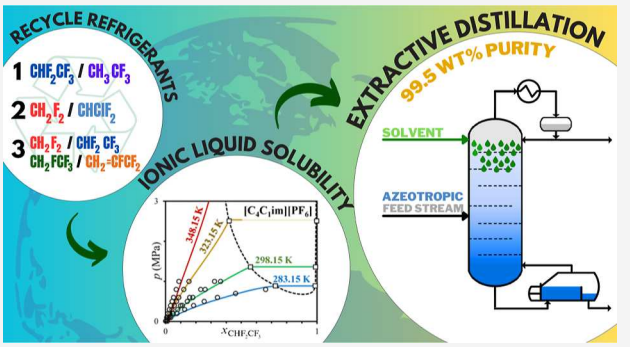

1. INTRODUCTION

Chlorofluorocarbons (CFCs) and hydrochlorofluorocarbons (HCFCs) have been used as refrigerants since the 1930s but were phased out of production according to the Montreal Protocol in 1987 due to their high ozone depletion potential (ODP).[1,2] In 1990, the Significant New Alternatives policy (SNAP) implemented a new amendment to the Clean Air Act to further monitor the phase out of high ODP chemicals. Hydrofluorocarbons (HFCs), notable for having zero ODP, replaced CFCs and HCFCs. However, the high global warming potential (GWP) of HFCs warranted the Kigali Amendment to the Montreal Protocol in 2016.[3] This would phase out HFCs in favor of a fourth generation of refrigerants, hydrofluoroolefins (HFOs), which have zero ODP and a low GWP. In 2020, the United States passed the American Innovation and Manufacturing (AIM) Act, which requires the production and consumption of HFCs to decrease by at least 85% before 2036.[4] As the transition to HFOs continues, finding an alternative method for disposing and recycling HFCs is paramount so that high-GWP refrigerants are not incinerated or vented.[5] Instead of discarding the HFC mixtures as chemical waste, the low-GWP HFCs can be recycled into HFC/HFO blends, and the high-GWP HFCs can be used as chemical feedstocks for producing fluorinated polymers, electrolytes, and agriculture chemicals, just to name a few. Recycling HFCs proves to be difficult because these mixtures are azeotropic and cannot be separated using standard distillation methods; however, extractive distillation provides a solution.

Extractive distillation utilizes an entrainer (a second feed stream) to alter the volatility of the feed components and "break" the azeotrope. The entrainer is then recovered from the entrained component and recycled back into the extractive distillation unit. Since ionic liquids (ILs) are non-volatile and have negligible vapor pressures (from $<10^{-3}$ to 10^{-5} Pa),[6−8] only a single-stage separation, such as a flash unit, is required to recycle the ionic liquid.

Previous works have shown that ILs have a high selectivity for many HFC mixtures, proving to be good candidates for extractive distillation.[9] Process simulations were developed for binary, ternary, and multicomponent refrigerant mixtures but only with ILs 1-butyl-3-methylimidazolium hexafluorophosphate ($[C_4C_1im][PF_6]$) and 1-ethyl-3-methylimidazolium *bis*(trifluoromethylsulfonyl)imide ($[C_2C_1im][Tf_2N]$).[10−12] It was concluded that binary mixtures such as difluoromethane/chlorodifluoromethane (HFC-32/HCFC-22) and pentafluoro-

Received: June 28, 2023
Revised: August 30, 2023
Accepted: September 1, 2023
Published: September 19, 2023

ethane/1,1,1-trifluoroethane (HFC-125/HFC-143a) require a more selective IL to achieve separations of 99.5 wt %.

The refrigerant industry has potential to transition to HFOs exclusively; therefore, the separation of the HFC/HFO mixtures will also be investigated. Examples of the commercial HFC/HFO mixture refrigerants are listed in Table 1, and

Table 1. Commercial HFO/HFC Blends

refrigerant		components
binary		
R-450	A	HFC-134a/HFO-1234ze(E)
R-451	A/B	HFC-134a/HFO-1234yf
R-454	A/B/C	HFC-32/HFO-1234yf
R-513	A/B	HFC-134a/HFO-1234yf
R-515	A	HFC-227ea/HFO-1234ze(E)
ternary		
R-444	A/B	HFC-32/HFC-152a/HFO-1234ze(E)
R-445	A	HFC-134a/HFO-1234ze(E)/CO_2
R-446	A	HFC-32/HFO-1234ze(E)/HC-600
R-447	A/B	HFC-32/HFC-125/HFO-1234ze(E)
R-452	A/B/C	HFC-32/HFC-125/HFO-1234yf
R-455	A	HFC-32/HFO-1234yf/CO_2
R-456	A	HFC-32/HFC-134a/HFO-1234ze(E)
R-457	A	HFC-32/HFC-152a/HFO-1234yf
R-459	A/B	HFC-32/HFC-1234yf/HFC-1234ze(E)
R-465	A	HFC-32/HFO-1234yf/HC-290
R-516	A	HFC-134a/HFC-152a/HFO-1234yf
multi-component		
R-448	A	HFC-32/HFC-125/HFC-134a/ HFO-1234yf/HFC-1234ze(E)
R-449	A/B/C	HFC-32/HFC-125/HFC-134a/HFO-1234yf
R-460	A/B/C	HFC-32/HFC-125/HFC-134a/HFC-1234ze(E)
R-463	A	HFC-32/HFC-125/HFC-134a/HFO-1234yf/CO_2
R-464	A	HFC-32/HFC-125/HFC-227ea/HFC-1234ze(E)

details on the various compositions are provided in the Supporting Information in Table S1. The commonly used components in these mixtures include HFC-32, HFC-125, 1,1,1,2-tetrafluoroethane (HFC-134a), 2,3,3,3-tetrafluoropropene (HFO-1234yf), 1,1-difluoroethane (HFC-152a), 1,1,1,2,3,3,3-heptafluoropropane (HFC-227ea), propane (HC-290), butane (HC-600), 1,3,3,3-tetrafluoropropene [HFO-1234ze(E)], and carbon dioxide (CO_2). For the general representation of the common HFC/HFO blends, a mixture of 25 wt % HFC-32, 25 wt % HFC-125, 25 wt % HFC-134a, and 25 wt % HFO-1234yf (mixture R-449A) is selected for modeling the separation.

Developing a simulation requires regressing the experimental data for both IL solubility and binary refrigerant equilibrium. A review of all equilibrium and mass transport experimental data for refrigerant solubility in ILs has been published and is used to determine the different entrainer candidates; though Henry's constants are provided, the solubility data must be regressed to predict the equilibrium at varying temperatures and pressures for each binary system.[13] All ILs with available solubility data for each of the components in the three mixtures are summarized in Table 2, resulting in nine different ILs and thirty-four binary mixtures; the non-abbreviated names for these ILs are provided in Table S2. Additionally, the regression results from our previous work for all HFC and HFC/HCFC equilibria are included in this work.[10] Since our prior research did not regress the binary interaction parameters

Table 2. List of the ILs Available for Each Mixture

mixture	IL
HFC-32/HCFC-22	$[C_2C_1im][Tf_2N]$
	$[C_2C_1im][TFES]$
	$[C_4C_1im][BF_4]$
	$[C_4C_1im][PF_6]$
HFC-125/HFC-143a	$[C_4C_1im][PF_6]$
	$[C_6C_1im][Tf_2N]$
	$[P_{(14)666}][TMPP]$
HFC-32/HFC-125	$[C_2C_1im][Ac]$
HFC-134a/HFO-1234yf	$[C_2C_1im][OTf]$
	$[C_2C_1im][Tf_2N]$
	$[C_2C_1im][SCN]$
	$[C_4C_1im][PF_6]$
	$[C_6C_1im][Tf_2N]$

for HFC-32, HFC-125, and HFC-134a with HFO-1234yf, the binary interaction parameters were retrieved from the studies of other groups[14] (currently the only study with binary equilibrium data for HFC-125/HFO1234yf and HFC-134a/HFO1234yf, along with only one other source for HFC-32/HFO-1234yf[15]).

This work is a continuation of our previous work to find a suitable IL entrainer for the separation of azeotropic binary systems HFC-125/HFC-143a and HFC-32/HCFC-22, with the addition of IL selection for separating the HFC/HFO system of HFC-32, HFC-125, HFC-134a, and HFO-1234yf. The experimental data for the binary systems in Table 2 are regressed to predict the entire composition range; then, an IL entrainer is selected for each system. A process design is developed using extractive distillation with a flash unit solvent recovery to achieve 99.5 wt % of each component. The three necessary steps in developing a process design are as follows: (i) regressing experimental vapor−liquid equilibrium (VLE) and liquid−liquid equilibrium (LLE) data to predict the phase behavior over the entire composition range, (ii) creating a simulation method with defined constraints and heuristics, and (iii) finding the optimal parameters in achieving the target purity (99.5 wt %).

2. METHODS

The phase equilibrium is achieved when the chemical potential of a component, i, is equal in each phase; this can also be defined as the mixture fugacity of phase one, $\overline{f}_i^{\mathrm{I}}$, equaling the mixture fugacity of phase two, $\overline{f}_i^{\mathrm{II}}$; $\overline{f}_i^{\mathrm{I}}(T, P, x^{\mathrm{I}}) = \overline{f}_i^{\mathrm{II}}(T, P, x^{\mathrm{II}})$. The mixture fugacity can be further defined with an activity coefficient model using the $\gamma-\varphi$ method or equation of state (EoS) via the $\varphi-\varphi$ method. The literature review in our previous work showed that most process design publications with IL entrainers use the non-random two-liquid activity coefficient model while assuming the vapor phase to be ideal ($\varphi^{\mathrm{V}} = 1$).[10] For halogenated polar compounds (such as HFCs and HFOs) and components near their critical point (such as gas solubility in ILs at high temperatures or pressures), the ideal gas mixture in the vapor phase is not a good assumption. Therefore, the $\varphi-\varphi$ method is necessary, and an EoS is selected for reliable vapor phase calculations.

The vapor and liquid phase equilibria for all binary systems are modeled with the Peng−Robinson EoS(PR-EoS),[16,17]

https://doi.org/10.1021/acs.iecr.3c02180
Ind. Eng. Chem. Res. 2023, 62, 16070−16080

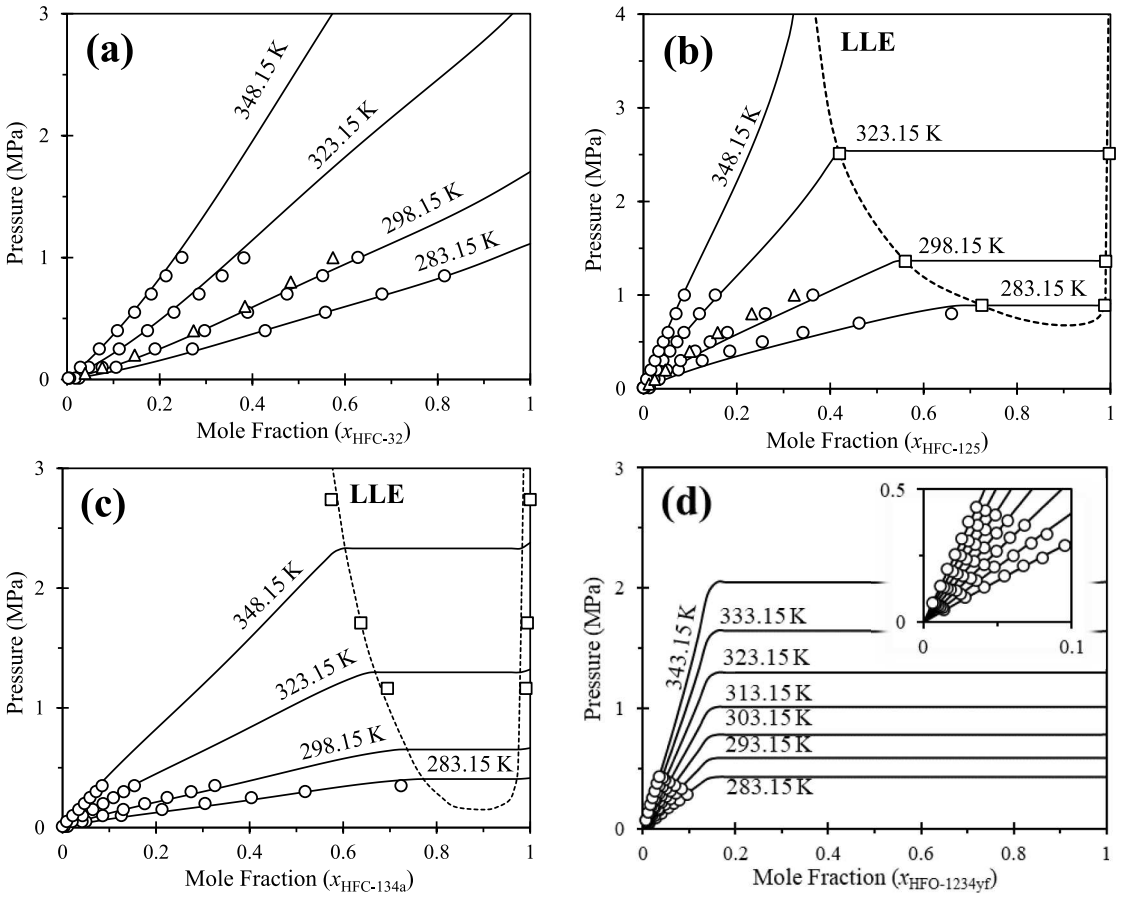

Figure 1. *PTx* data (○, Δ) for (a) HFC-32,[9,27] (b) HFC-125,[9,27] (c) HFC-134a,[9,25] and (d) HFO-1234yf[28] with $[C_4C_1im][PF_6]$ and corresponding LLE data (□) for HFC-125 and HFC-134a.

shown in eq 1, by regressing experimental VLE and LLE data. All regressions are conducted using the Aspen Plus software.

$$P = \frac{RT}{\underline{V} - b} - \frac{a}{\underline{V}(\underline{V} + b) + b(\underline{V} - b)} \tag{1}$$

The PR-EoS parameters a and b are a function of pure component critical properties: critical temperature (T_c), critical pressure, (P_c), and acentric factor (Ω). These properties, as well as the boiling temperature (T_b), molecular weight (MW), critical volume or compressibility factor (V_c or Z_c), and ideal gas heat capacities ($\Delta C_{P,IG}$), are required to regress PR-EoS using Aspen Plus. Ionic liquid critical properties and T_b are pseudo-properties since ILs do not vaporize and will decompose before reaching critical conditions. Group contribution methods are used to predict the critical properties, including Ω and T_b[18,19] and $\Delta C_{P,IG}$[20] as a function of T for all ILs investigated in this work and are provided in Tables S2 and S3.

To define the multicomponent equilibrium for an EoS, a mixing rule must be selected to redefine the pure component parameters a and b into the mixing parameters a_m and b_m. The van der Waal's 1-parameter (vdW1) mixing rule, shown in eqs 2 and 3, is used to regress all the HFC and HFC/HFO properties, and experimental VLE data is fit to the temperature-dependent binary interaction parameter, k_{ij}, shown in eq 4. The interaction parameter is assumed to be symmetric ($k_{ij} = k_{ji}$).

$$a_m = \sum_{i=1}^{C}\sum_{j=1}^{C} x_i x_j (1 - k_{ij})(a_i a_j)^{0.5} \tag{2}$$

$$b_m = \sum_{j}^{C} x_i b_i \tag{3}$$

$$k_{ij} = k_{ij}^{(1)} + k_{ij}^{(2)} T \tag{4}$$

For highly non-ideal systems with asymmetric mixing rules, such as IL solubility, the Boston−Mathias (B−M)[17] correction can be added to the vdW1, as shown in eq 5, where a_0 represents the vdW1 mixing rule from eq 2 and a_1 represents the B−M correction given in eq 6. This method provides a second binary interaction parameter for regression, l_{ij}, which has proven to be necessary when modeling solubility in ILs as discussed in our previous work.[10] The parameter l_{ij} carries the same linear temperature-dependency as parameter k_{ij} (shown in eq 4) and is regressed asymmetrically ($l_{ij} \neq l_{ji}$).

$$a_m = a_0 + a_1 \tag{5}$$

$$a_1 = \sum_{i=1}^{c} x_i \left\{ \sum_{j=1}^{c} x_j [(a_i a_j)^{0.5}] \right\}^3 \tag{6}$$

The regression method first regresses parameters $k_{ij}^{(1)}$ and $k_{ij}^{(2)}$, followed by parameters $l_{ij}^{(1)}$ and $l_{ji}^{(1)}$, and finally parameters $l_{ij}^{(2)}$ and $l_{ji}^{(2)}$. Temperature-dependent parameters

https://doi.org/10.1021/acs.iecr.3c02180
Ind. Eng. Chem. Res. 2023, 62, 16070−16080

$k_{ij}^{(2)}$ and $l_{ij}^{(2)}$ are only regressed if multiple isotherms are available in the VLE data.

The maximum likelihood (ML) technique[21] is selected for regressing the experimental data and weighs the objective function by the error (σ) in each experimental coordinate. Errors are assumed to be similar for all datasets with the following values: σ_T = 0.1 K, σ_P = 0.1% MPa, σ_x = 0.1 mol %, and σ_y = 1.0 mol %. The average absolute deviation (AAD) values are calculated for each experimental variable (T, P, x_i, y_i), and each dataset is analyzed individually.

3. REGRESSION

3.1. PTx Diagrams. Experimental *PTx* data of refrigerant solubility in ILs are fit to the PR-EoS by the regressing parameters k_{ij} and l_{ij} with the vdW1 and B−M mixing rule. In this work, a total of forty-nine datasets for thirty-four binary mixtures are regressed. Though there are multiple datasets for the same binary system, not all data are added to the regression when calculating k_{ij} and l_{ij}. However, all the datasets are included in the *PTx* diagrams at the same isotherms for comparison.

An example of a regression fit for the solubility of multiple refrigerants in one IL can be seen in Figure 1, in which one or more datasets define the equilibrium of HFC-32, HFC-125, HFC-134a, and HFO-1234yf with $[C_4C_1im][PF_6]$ at various temperatures (i.e., isotherms). The liquid−liquid equilibrium region occurs when the solubility trend exceeds the vapor pressure of the pure refrigerant; this is seen with the solubility systems HFC-125, HFC-134a, and HFO-1234yf (Figure 1b−d). The solubility of HFC-125 and HFC-134a had experimental data to confirm the LLE region, while HFO-1234yf predicted LLE (displayed with the horizonal lines), but no experimental data are available to confirm where the LLE region exists.

When LLE data is not included in the regression, the PR-EoS either over- or under-estimates the LLE region; therefore, *PTx* diagrams that predict an LLE region without confirmation of the experimental data should be considered with caution. For all 34 binary systems, the only systems with LLE data available include the following: HFC-125[22] and HFC-134a[23] with $[C_2C_1im][Tf_2N]$; HFC-125,[24] HFC-134a, and HFC-143a with $[C_4C_1im][PF_6]$;[25] and one data point for HFC-134a with $[C_6C_1im][Tf_2N]$.[26] For the best LLE prediction, the liquid phase data points (<90 mol %) were regressed, while the higher concentration liquid phase data points (>95 mol %) were typically excluded. In a couple of cases, including the higher concentration liquid phase data points would result in unrealistic LLE regions and were therefore discarded.

Once experimental data is regressed and produces a satisfactory fit across the composition range for each refrigerant, a *PTx* comparison diagram is created to show the refrigerant solubility differences at one isotherm (i.e., 298.15 K), as shown in Figure 2. When analyzing the lower composition range of the refrigerant ($x \leq 0.3$), $[C_4C_1im][PF_6]$ shows a high solubility difference and good selectivity for the separation of HFC-32/HFC-125 and HFC-134a/HFO-1234yf. However, $[C_4C_1im][PF_6]$ shows a poor selectivity for HFC-32/HFC-134a and HFC-125/HFO-1234yf.

PTx comparison diagrams help determine the light key (LK) and heavy key (HK) components when using extractive distillation; in this case, for the extractive distillation with the entrainer $[C_4C_1im][PF_6]$, the more soluble components, HFC-32 and HFC-134a, are expected to be the HK and leave in the bottom stream with the IL, while HFC-125 and HFO-1234yf are expected to be the LK and leave in the distillate stream.

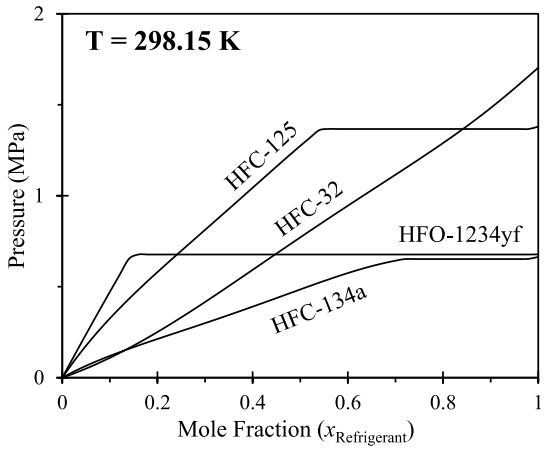

Figure 2. *PTx* comparison for HFC-32, HFC-125, HFC-134a, and HFO-1234yf in $[C_4C_1im][PF_6]$ at 298.15 K.

All *PTx* diagrams of the experimental data compared to the regression fit and *PTx* comparison diagrams (in both mole and mass fraction) can be found in the Supporting Information from Figures S1 to S13. The summary of the regression results for parameters k_{ij} and l_{ij} and the AAD of T, P, and x_i for each dataset are also displayed in Tables S4, S5, and S6.

3.2. Selecting an IL. Three different methods were tested to numerically define the ILs which had the highest selectivity to be the best candidates for separation with extractive distillation: (i) ratio of pressure-over-composition slopes as $x \rightarrow 0$, (ii) ratio of solubilities at 0.1013 MPa, and (iii) ratio of solubilities at 0.50 MPa. Each method resulted in a different order of selectivity, and all solubilities were predicted at 298.15 K in units of mole fraction.

These methods were tested with the ILs listed for the HFC-32/HCFC-22 separation in an extractive distillation simulation, and the order of separation efficiency lined up with the ordering given by the ratio of solubilities at 0.50 MPa. Extractive distillation of the refrigerants requires a pressurized vessel to avoid low-temperature separation or cryogenic distillation, so comparing solubilities at elevated pressures rather than atmospheric pressures confirmed the hypothesis that the solubilities should be compared at conditions like those used in the unit operation.

For the binary mixture HFC-32/HCFC-22, the refrigerant composition/solubility is predicted at 0.50 MPa and 298.15 K for the ILs $[C_2C_1im][Tf_2N]$, $[C_2C_1im][TFES]$, $[C_4C_1im][BF_4]$, and $[C_4C_1im][PF_6]$, and the calculated selectivities are shown in Table 3. The order of ILs in terms of increasing

Table 3. Selectivities for HFC-32/HCFC-22 with ILs at P = 0.50 MPa and T = 298.15 K

IL	refrigerant (i)	100x	S_{ij}	ref
$[C_2C_1im][Tf_2N]$	HFC-32	39.8	1.374	30, 31
	HCFC-22	54.7		32
$[C_2C_1im][TFES]$	HFC-32	25.3	1.857	30
	HCFC-22	47.0		32
$[C_4C_1im][BF_4]$	HFC-32	31.9	1.578	9, 27
	HCFC-22	50.3		32
$[C_4C_1im][PF_6]$	HFC-32	34.8	1.376	9, 27
	HCFC-22	47.9		32

https://doi.org/10.1021/acs.iecr.3c02180
Ind. Eng. Chem. Res. 2023, 62, 16070−16080

selectivity for the separation of HFC-32/HCFC-22 is $[C_2C_1im][Tf_2N]$ < $[C_4C_1im][PF_6]$ < $[C_4C_1im][BF_4]$ < $[C_2C_1im]$[TFES], with HFC-32 being consistently more soluble than HCFC-22. Based on these results, $[C_2C_1im]$-[TFES] is selected for the separation of HFC-32/HCFC-22. This IL has a viscosity of 0.0117 ± 0.0056 Pa·s at a temperature of 293.15 K and a pressure of 0.1013 MPa.[29]

For the next binary mixture of HFC-125/HFC-143a, the selectivities of $[C_4C_1im][PF_6]$, $[C_6C_1im][Tf_2N]$, and $[P_{(14)666}]$[TMPP] are shown in Table 4. The order of ILs in terms of increasing selectivity for the separation of HFC-125/HFC-143a is $[C_4C_1im][PF_6]$ < $[C_6C_1im][Tf_2N]$ < $[P_{(14)666}]$-[TMPP] with HFC-125 being consistently more soluble than HFC-143a. Based on these results, $[P_{(14)666}]$[TMPP] is selected for the separation of HFC-125/HFC-143a. This IL has a viscosity of 1.058 ± 0.091 Pa·s at a temperature of 298.15 K and a pressure of 0.1013 MPa.[33]

Table 4. Selectivities for HFC-125/HFC-143a with ILs at P = 0.50 MPa and T = 298.15 K

IL	refrigerant (i)	100x	S_{ij}	ref
$[C_4C_1im][PF_6]$	HFC-125	16.7	1.421	9,24,27
	HFC-143a	11.7		9,25
$[C_6C_1im][Tf_2N]$	HFC-125	35.3	1.426	22
	HFC-143a	24.8		34
$[P_{(14)666}]$[TMPP]	HFC-125	63.7	2.149	35
	HFC-143a	29.6		35

The final analysis for IL selection is done on the separation of HFC-32, HFC-125, HFC-134a, and HFO-1234yf. When separating three or more components, the first necessary step is to test if conventional distillation can achieve separation between the multicomponent mixture by creating a mass distilled versus distillate rate diagram (introduced in previous work).[10] This diagram is created for the equimass system of HFC-32, HFC-125, HFC-134a, and HFO-1234yf and is shown in Figure S14. Since HFC-32 and HFC-125 can be separated from HFC-134a and HFO-1234yf using conventional distillation, and neither HFC-32 nor HFC-125 form an azeotrope with HFC-134a or HFO-1234yf, the IL selectivities are calculated for the binary mixtures of HFC-32/HFC-125 and HFC-134a/HFO-1234yf and are shown in Table 5.

The order of ILs in terms of increasing selectivity for the separation of HFC-32/HFC-125 is $[C_6C_1im][Tf_2N]$ < $[C_2C_1im][Ac]$ < $[C_2C_1im][TF_2N]$ < $[C_2C_1im][OTf]$ < $[C_4C_1im][PF_6]$ < $[C_2C_1im][SCN]$. The IL $[C_2C_1im][Ac]$ is the only solvent where HFC-125 is more soluble than HFC-32 and results in a higher selectivity than $[C_6C_1im][Tf_2N]$. HFC-125 is more soluble than HFC-32 and is a rare case and has only been seen previously with $[C_4C_1im][Ac]$,[27] $[C_6C_1im]$-[Cl], and $[P_{(14)666}]$[Cl].[46] The IL $[C_2C_1im][SCN]$ has the highest selectivity and is the IL of choice for the separation of HFC-32/HFC-125. This IL has a viscosity of 0.0245 ± 0.0003 Pa·s at a temperature of 298.15 K and a pressure of 0.1013 MPa.[47]

The order of selectivity for the separation of HFC-134a/HFO-1234yf is $[C_6C_1im][Tf_2N]$ < $[C_2C_1im][Tf_2N]$ < $[C_2C_1im][OTf]$ < $[C_4C_1im][PF_6]$ < $[C_2C_1im][SCN]$ < $[C_2C_1im][Ac]$ with HFC-134a being more soluble than HFO-1234yf. Even though $[C_2C_1im][Ac]$ has the highest selectivity for the HFC-134a/HFO-1234yf system, this IL is not considered due to its low thermal stability and the chemical complex it forms with CO_2.[48−52]

Table 5. Selectivities for HFC-32/HFC-125 and HFC-134a/HFO-1234yf with ILs at P = 0.50 MPa and T = 298.15 K

IL	refrigerant (i)	100x	S_{ij}	ref
$[C_2C_1im][Ac]$	HFC-32	22.8	0.669	31
	HFC-125	34.1	(1.495)	31
	HFC-134a	31.0	7.410	31
	HFO-1234yf	4.19		36
$[C_2C_1im][OTf]$	HFC-32	26.6	1.502	31,37,38
	HFC-125	17.7		31
	HFC-134a	41.2	4.266	31,38
	HFO-1234yf	9.66		38
$[C_2C_1im][SCN]$	HFC-32	13.8	6.180	39
	HFC-125	2.24		40
	HFC-134a	9.18	5.018	39
	HFO-1234yf	1.83		39
$[C_2C_1im][TF_2N]$	HFC-32	39.8	1.497	30,31
	HFC-125	26.6		31,41
	HFC-134a	62.0	2.704	31,42−44
	HFO-1234yf	22.9		38
$[C_4C_1im][PF_6]$	HFC-32	34.8	2.087	9,27
	HFC-125	16.7		9,24,27
	HFC-134a	51.6	4.860	9,25
	HFO-1234yf	10.6		28
$[C_6C_1im][Tf_2N]$	HFC-32	44.9	1.271	22
	HFC-125	35.3		22
	HFC-134a	67.1	1.892	23,26
	HFO-1234yf	35.5		45

In both binary systems, $[C_6C_1im][Tf_2N]$ is determined to be the least selective IL. Previous extractive distillation simulations have shown that for the separation of HFC-32/HFC-125, $[C_4C_1im][PF_6]$ (S_{ij} = 2.09) is able to achieve 99.5 wt % purity within the system constraints while $[C_2C_1im]$-$[Tf_2N]$ (S_{ij} = 1.50) cannot, so we assume ILs with S_{ij} > 1.80 are suitable entrainers to achieve 99.5 wt % separation. This means that all the candidates regressed for HFC-134a/HFO-1234yf are potential candidates for this separation.

4. SIMULATION

The required unit operations for the separation of multicomponent refrigerant mixtures are as follows: (i) conventional distillation for non-azeotropic mixtures, (ii) extractive distillation with a selective solvent for azeotropic mixtures, and (iii) flash separation for the single-stage IL solvent recovery. To run a simulation in Aspen Plus for a distillation process, the following variables are required: distillate rate (D), operating pressure (P), total number of theoretical stages (N_T), feed stage (N_F), reflux ratio (RR), feed temperature (T_F), and feed pressure (P_F). Extractive distillation also includes the following additional variables: solvent feed stage (N_S), solvent-to-feed (S/F) ratio, solvent feed temperature (T_S), and solvent feed pressure (P_S).

To limit the number of variables in the optimization, heuristics are first defined:

1. The distillate rate (D) should equal the feed rate (F) of the LK component(s) to achieve a complete component recovery at the desired purity.
2. The liquid-phase feed will result in a higher distillate purity than that of a vapor-phase feed, and cooler feed streams (T_F and T_S) result in higher distillate purity.

https://doi.org/10.1021/acs.iecr.3c02180
Ind. Eng. Chem. Res. 2023, 62, 16070−16080

This is believed to decrease the overall temperature of the column profile and increase the selectivity at each equilibrium stage.

3. Since N_S is a function of the feed component's volatility and IL solvents are non-volatile, the solvent should enter at the top of the column (N_S = 2).

All the feed temperatures are set to 293.15 K (ambient temperature), so no additional cooling of the streams is necessary. The feed pressure is set at 2.0 MPa (or higher) to be above the column operating pressure and to ensure the feed is in the liquid state.

The variables P, N_T, N_F, RR, and S/F are then optimized to obtain the highest component purities within the defined constraints. The column operating pressure is constrained for the condenser to operate with chilled water (i.e., T_{Cond} > 293.15 K) and the reboiler temperature to avoid the potential issues with IL decomposition (i.e., T_{Reb} < 423.15 K). At each selected N_T, the N_F is optimized to find the greatest distillate purity; N_F is influenced by the mole flow ratio of the LK and HK component(s) at each stage. Since all the feed fractions are specified at 50/50 wt % mixture and the molecular weights of the feed components are similar, all the results showed the optimal N_F to be at N_F/N_T = 50%. The reflux ratio (RR) is the amount of distillate recycled into the column through the N_T; this can reduce the N_T required to obtain the required purity but will ultimately reach a plateau at RR ≤ 5. The RR is varied from 0.5 to 5. The S/F is varied from 0.5 to 10. The large values for the S/F indicate an inefficient separation and that the selectivity is low.

The relationships of these variables are also important to consider when developing a simulation method. The S/F improves the selectivity of components, thus reducing the N_T, so increasing the S/F will decrease the N_T required to achieve purity but will increase the reboiler heat duty, Q_{Reb}, and temperature, T_{Reb}. Increasing the S/F will also increase the optimum P and the amount of the HK (solute), but increasing P will also increase the Q_{Reb}, T_{Reb}, and T_{Cond} and will decrease the Q_{Cond}. When all the parameters are consistent, a lower N_T will decrease the optimal RR, which will ultimately decrease the Q_{Cond}. The P, RR, and S/F have little effect on the optimal N_F, but increasing the amount of the LK (distillate component) will increase the optimal N_F. These relationships are further discussed for the HFC-125/HFC-143a separation in the following section.

The optimization process follows the order: $D \rightarrow S/F \rightarrow N_T \rightarrow P \rightarrow N_F \rightarrow$ RR. Since the feed rate is known, D could be determined; then, S/F was initially set to 1 and N_T to 20. The LK components will determine T_{Cond} at different pressures, and the HK and S/F will determine T_{Reb} to define the range of P; thus, the optimization and range for P must be determined after D is defined and S/F is selected. Next, the N_F and RR were varied to obtain the maximum distillate purity. If the desired purity (i.e., 99.5 wt %) could not be achieved, then the N_T was increased, and the optimization process was repeated. If N_T > 50, then the S/F was increased. Once the desired purity is achieved, the minimum Q_{Reb} is determined by optimizing the P and S/F ratio at a specified product purity.

A flash vessel, single-stage equilibrium process only dependent on T and P, is used for recovering and recycling the IL back to the extractive distillation column. Since ILs are non-volatile, only a single-stage separation is required to remove the refrigerant. The heat duty of the flash vessel, Q_{flash}, is set to zero, and the heat of vaporization determines the operating T. Typically, vacuum conditions are required to extract all the HK before the IL can be recycled back into the extractive distillation column. In this paper, the simulations are tested with a flash vessel at both vacuum (P = 0.01 MPa) and atmospheric conditions (P = 0.1013 MPa) to see if the IL is selective enough to separate refrigerants at the desired purity, while a small amount of refrigerant remains in the recycle stream. For practical application, a small amount of refrigerant (w_{ref} < 0.5 wt %) remaining in the recycled IL is beneficial to decrease the viscosity of the fluid and reduce the pumping power.

If the process does not achieve a satisfactory purity within the constraints of the system, additional methods for improving the distillate purity include increasing the pressure by broadening the constraints of the T_{Cond} and T_{Reb}, increasing N_T above 50, or increasing the S/F ratio. Changing D will also improve the purity of one of the two components but will reduce the overall product recovery.

5. RESULTS

The process designs for the separation of azeotropic binary systems HFC-32/HCFC-22 and HFC-125/HFC-143a are developed to achieve 99.5 wt % purity of each component in the Aspen Plus simulation software. The process flow diagrams (PFDs) include an extractive distillation column, a flash vessel, a pump to recycle the solvent from the flash vessel to the column, and a solvent heat exchanger to cool the IL back to ambient temperatures (293.15 K). The IL, after being fed through the extractive distillation column, is recovered in a flash unit, and all IL is recycled in the system. The PFDs provide the mass fractions (w_i), mass flow rates (F, S, B_n, and D_n), heat duties (Q), T, P, RR, feed locations (N_S and N_F), and the number of theoretical stages (N_T).

The PFD includes an "OUT" stream leaving and reentering the flash vessel to represent the trace amount of IL in the refrigerant vapor stream (similar to how a demister would be used if IL were entrained in the refrigerant vapor). This is required because the PR-EoS overpredicts the vapor pressure for the IL.

Other works have used two flash units in series (the first at atmospheric pressure and the next at vacuum) to demonstrate the necessity of the vacuum conditions to fully recover the refrigerant from the IL entrainer, but in these simulations, one flash unit is used, and the systems are initially tested with the flash unit at vacuum or atmospheric pressure. The process designs follow the progression of (i) solvent recovery at vacuum conditions (P = 0.01 MPa), (ii) increase the S/F to lower N_T, and if separation can be completed with a vacuum flash vessel with a reasonable S/F and N_T, then (iii) solvent recovery at atmospheric conditions (P = 0.1013 MPa).

5.1. HFC-125/HFC-143a with [$P_{(14)666}$][TMPP]. A feed composition of 50/50 wt % of HFC-125 and HFC-143a is fed into an extractive distillation column at F = 10 kg/h, and the distillate rate of the column is set to D = 5 kg/h to optimize the variables at maximized separation (e.g., 99.5 wt % purity and recovery). Both the IL solvent and refrigerant feed enter the column at 293.15 K. The solvent for this separation is [$P_{(14)666}$][TMPP] that is selective to absorbing HFC-125; therefore, HFC-143a is the LK and is collected in the distillate stream, while HFC-125 is the HK and is passed through the reboiler to the flash vessel to be collected in the vapor stream.

https://doi.org/10.1021/acs.iecr.3c02180
Ind. Eng. Chem. Res. 2023, 62, 16070−16080

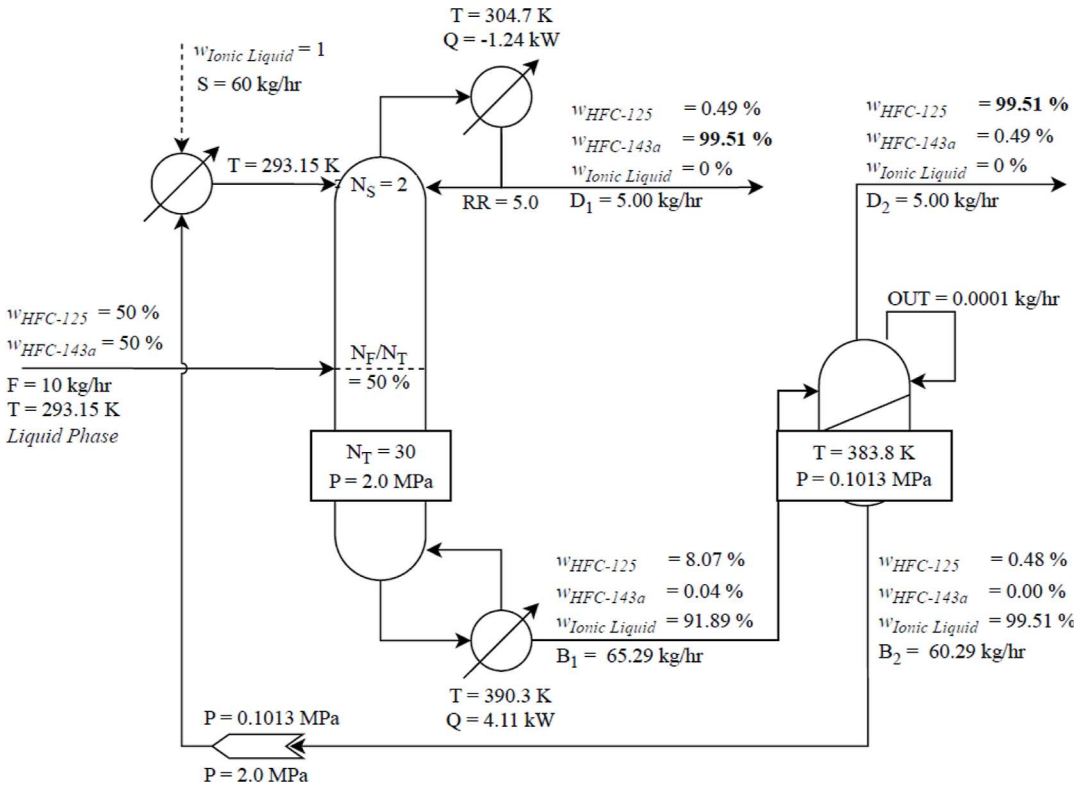

Figure 3. Process design of separating HFC-125/HFC-143a in extractive distillation with the solvent $[P_{(14)666}][TMPP]$ and a flash recovery unit at P = 0.1013 MPa.

For the preliminary process design, the flash unit for solvent recovery operates at vacuum (0.01 MPa) to extract nearly all the absorbed refrigerant, HFC-125, and minimize the refrigerant in the solvent recycle stream; these results are available in the Supporting Information in Figure S15. This system can achieve the target purity with the extractive distillation column operating at P = 1.2 MPa and S/F = 4 with N_T = 38 (purity cannot be achieved with S/F = 3 with $N_T \leq 50$ and RR $\leq$ 5.0). A sensitivity analysis showed that the optimal pressure to maximize the distillate purity with S/F = 4 is at 0.7 MPa, but this would result in very cold condenser temperatures, so the column pressure is increased to P = 1.2 MPa to ensure T_{Cond} > 293.15 K. With S/F = 4 and P = 1.2 MPa, the reboiler operated at T_{Reb} = 359.4 K and Q_{Reb} = 2.36 kW. The optimal feed stage is at N_F/N_T = 50% as expected. The reflux ratio is then varied from 0.0 to 5.0, and the purity of HFC-143a reaches a maximum at about RR = 4.0 resulting in Q_{Cond} = −1.14 kW.

The solvent and the absorbed refrigerant, HFC-125, leave the reboiler and are fed into an adiabatic flash unit for solvent recovery, and the flash unit's overall temperature decreased from 359.4 to 347.5 K with the heat of vaporization of the refrigerant leaving the IL. A trace amount of 0.0001 kg/h of IL is found in the vapor stream, which is separated using a demister and is recycled back into the flash unit with the liquid stream. The solvent recycle stream contains 0.0375 kg/h HFC-125 and 0.0001 kg/h HFC-143a.

In the next process design, the S/F is increased from 4 to 5 to improve the separation efficiency and decrease the overall N_T; this simulation also includes a vacuum flash unit for solvent recovery and the same constraints of RR $\leq$ 5.0 and T_{Cond} > 293.15 K and T_{Reb} < 373.15 K. These results are shown in the Supporting Information in Figure S16. The system achieved purity with N_T = 28 with 10 less stages. The optimal pressure for S/F = 5 is at P = 0.9 MPa, but the column pressure is set to 1.2 MPa to ensure T_{Cond} > 293.15 K. The system purity reached a maximum at about RR = 2.0. A lower N_T will decrease the optimal RR, which will ultimately decrease the Q_{Cond}. Though this system reached purity with a much lower Q_{Cond} = −0.69 kW, increasing the S/F to 5 increased the Q_{Reb} from 2.36 to 2.51 kW. The solvent recycle stream contained 0.0347 kg/h HFC-125 and 0.0001 kg/h HFC-143a, which is slightly lesser recycled refrigerant than that in the previous process design because of the higher flash temperature of 361.4 K.

For the final process design, the flash unit for solvent recovery operates at atmospheric pressure (0.1013 MPa) to determine if the refrigerant purity specifications (99.5 wt %) can be achieved with the higher amount of the HK refrigerant in the solvent recycle stream. These results are shown in Figure 3. The extractive distillation column operates at P = 1.5 MPa, which is the optimal pressure at S/F = 6 and N_T = 30. Even though N_T = 30 is between the value for the other two process designs, the purity of HFC-143a reached a maximum at RR = 5.0 (a much higher RR than the two previous simulations), resulting in Q_{Cond} = −1.24 kW. This indicates that N_T influences not only the optimal RR but also the recycle stream composition. The product stream leaving the distillate of the extractive distillation column is 99.51 wt % HFC-143a and 0.49 wt % HFC-125.

The reboiler operated at T_{Reb} = 390.3 K and Q_{Reb} = 4.11 kW, and the solvent and the absorbed refrigerant, HFC-125, leave the reboiler and are fed into an adiabatic flash unit for solvent recovery. After heat of vaporization, the flash vessel temperature decreased from 390.3 to 383.8 K. A trace amount of 0.0001 kg/h IL is found in the vapor stream and is separated

https://doi.org/10.1021/acs.iecr.3c02180
Ind. Eng. Chem. Res. 2023, 62, 16070−16080

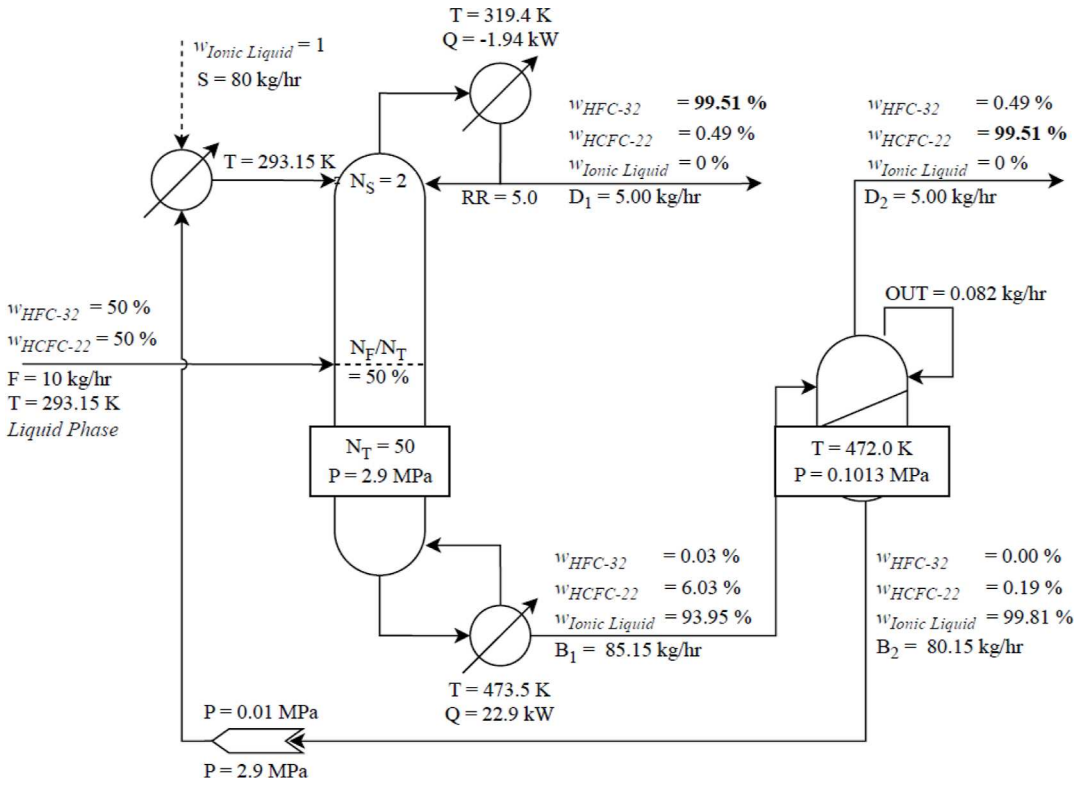

Figure 4. Process design of separating HFC-32/HCFC-22 in extractive distillation with the solvent $[C_2C_1im][TFES]$ and a flash recovery unit at P = 0.1013 MPa.

and recycled into the liquid stream. With the ambient pressure limiting the total HFC-125 being extracted from the flash vessel, 0.292 kg/h HFC-125 and 0.001 kg/h HFC-143 are recycled back with the solvent stream, which is about ten times the recycled amount of refrigerant compared to that in the vacuum flash vessel. The product stream leaving the flash vessel is 99.51 wt % HFC-125 and 0.49 wt % HFC-143a.

5.2. HFC-32/HCFC-22 with $[C_2C_1im][TFES]$. A feed composition of 50/50 wt % HFC-32 and HCFC-22 is fed into an extractive distillation column at F = 10 kg/h, and the distillate rate of the column is set to D = 5 kg/h. Both the IL solvent and refrigerant feed entered the column at 293.15 K. The solvent for this separation is $[C_2C_1im][TFES]$, which is selective to absorbing HCFC-22. HCFC-22 is the HK, and HFC-32 is the LK.

For the preliminary process design, the flash unit for the solvent recovery operates at vacuum (0.01 MPa), and the results are shown in Figure S17 in the Supporting Information. This system achieves 99.51 wt % HFC-32 purity with an extractive distillation column operating at P = 1.5 MPa (to condense HFC-32 at T_{Cond} > 293.15 K) with S/F = 2 and N_T = 43; the reboiler operated at T_{Reb} = 342.45 K and Q_{Reb} = 3.27 kW, and the flash vessel operated at 331.2 K. The solvent recycle stream contained 0.0272 kg/h of HCFC-22 and 0.0001 kg/h of HFC-32. With increasing the S/F to 4, the system can also achieve purity with N_T = 35with 7 less stages. Increasing the S/F has less of an effect on N_T compared to that in the previous section (10 less N_T) because this solvent, $[C_2C_1im][TFES]$, has lower selectivity (S_{ij} = 1.857 vs S_{ij} = 2.149).

Since this process is able to achieve 99.51 wt % HFC-32 and 99.51 wt % HCFC-22 purities in both distillate and flash vapor streams, respectively, the final process design has the flash unit for solvent recovery operating at atmospheric pressure (0.1013 MPa) as shown in Figure 4. The extractive distillation column operated at P = 2.9 MPa, which is the optimal pressure at S/F = 8 and required N_T = 50 and RR = 5 with Q_{Cond} = −1.24 kW. Increasing RR slightly increases the purity because both N_T and S/F are high. This pressure also exceeded the reboiler constraint of T_{Reb} < 423.15 K, and the reboiler operated at T_{Reb} = 473.5 K and Q_{Reb} = 22.9 kW. The product stream leaving the distillate of the extractive distillation column is 99.51 wt % HFC-32 and 0.49 wt % HCFC-22.

The solvent and the absorbed HCFC-22 leave the reboiler and are fed into an adiabatic flash unit for solvent recovery. The overall flash temperature decreased from 473.5 to 472.0 K, and 0.082 kg/h of IL is found in the vapor stream. At ambient pressure, 0.1541 kg/h of HCFC-22 and 0.0006 kg/h of HFC-32 are recycled back with the solvent stream. The product stream leaving the flash vessel is 99.51 wt % HCFC-22 and 0.49 wt % HFC-32.

6. CONCLUSIONS

The concern over high GWP refrigerants has led to environmental initiatives by governments to replace HFCs with a new generation of refrigerants, HFOs and HFO/HFC mixtures. Extractive distillation with IL entrainers proposes a valid option to separate and recycle pure HFCs and HFOs instead of disposing the refrigerant mixtures as chemical waste. Three refrigerant mixtures are investigated: HFC-32/HCFC-22, HFC-125/HFC-143a, and R-449A (HFC-32/HFC-125/HFC-134a/HFC-1234yf).

ILs with available solubility data for the components in each of the three mixtures are investigated as potential candidates for an extractive distillation solvent and are regressed with the Peng−Robinson EoS, vdW1 mixing rule, and B−M correction factor, totaling in the regression of thirty-four binary mixtures

https://doi.org/10.1021/acs.iecr.3c02180
Ind. Eng. Chem. Res. 2023, 62, 16070−16080

with forty-nine datasets. Only six of the binary systems had experimental data to confirm the LLE regions, while seventeen binary systems predict an LLE region without confirmation and should be considered with caution. The summary of all the *PTx* diagrams of the experimental data compared to the regression fit, *PTx* comparison diagrams (in both mole and mass fraction), and regression results are provided in the Supporting Information.

Solubility comparisons and selectivities are determined using a simulation of the HFC-32/HCFC-22 with four IL candidates. Results show the separation efficiencies of the simulation matches the ratio of solubilities at 0.50 MPa, and the selectivities are calculated for all the ILs with the three refrigerant mixtures. Previous simulations and the process designs completed in this paper confirm that suitable entrainers for ILs must be $S_{ij} > 1.80$.

The IL $[C_2C_1im][TFES]$ is the selected solvent for the separation of HFC-32/HCFC-22, and $[P_{(14)666}][TMPP]$ is the selected solvent for the separation of HFC-125/HFC-143a. In these systems, HFC-32 and HFC-125 are the more soluble components and are the HK. For the multicomponent mixture of HFC-32, HFC-125, HFC-134a, and HFO-1234yf, a mass distilled versus distillate rate diagram is first created to test if conventional distillation can achieve separation between the components and confirmed that HFC-32 and HFC-125 (an azeotropic mixture) can be separated from HFC-134a and HFO-1234yf (another azeotropic mixture). The solvent selectivities are then provided for the binary mixtures HFC-32/HFC-125 and HFC-134a/HFO-1234yf, and $[C_2C_1im][SCN]$ is selected for both the systems. HFC-32 is consistently more soluble than HFC-125 except in the case of $[C_2C_1im][Ac]$, which is rare and is only found for three other ILs in the literature.

After the IL is selected, an optimization process is discussed by first defining the heuristics to limit the number of variables used in the optimization and then setting constraints for each variable in the extractive distillation column: $S/F \rightarrow N_T \rightarrow P \rightarrow N_F \rightarrow$ RR. Since ILs are non-volatile, only a single-stage separation is required to remove the refrigerant, and a flash vessel is operated at both vacuum (P = 0.01 MPa) and atmospheric conditions (P = 0.1013 MPa). The process designs and PFDs are developed for the separation of 50/50 wt % mixtures of HFC-32/HCFC-22 and HFC-125/HFC-143a to achieve 99.5 wt % purity of each component in Aspen Plus.

The binary mixture HFC-125/HFC-143a is separated using extractive distillation with $[P_{(14)666}][TMPP]$. The preliminary process design has the solvent recovery at vacuum conditions (P = 0.01 MPa) to minimize the refrigerant in the solvent recycle stream, and 99.51 wt % purity for both the refrigerants is achieved with P = 1.2 MPa, S/F = 4, and N_T = 38. The next process design demonstrates that increasing the S/F will decrease N_T, and 99.51 wt % of both the components is achieved with fewer N_T (P = 1.2 MPa, S/F = 5, and N_T = 28). The final design has the solvent recovery at atmospheric conditions (P = 0.1013 MPa), and 99.51 wt % of both components is achieved with P = 1.5 MPa, S/F = 6, and N_T = 30.

The binary mixture HFC-32/HCFC-22 is separated using extractive distillation with $[C_2C_1im][TFES]$. The preliminary process design has the solvent recovery at vacuum conditions (P = 0.01 MPa), and 99.51 wt % of both the components is achieved with P = 1.5 MPa, S/F = 2, and N_T = 43. Since $[C_2C_1im][TFES]$ has a lower selectivity than that of the HFC-125/HFC-143a separation with $[P_{(14)666}][TMPP]$, increasing the S/F has a smaller impact on decreasing the N_T (S_{ij} = 1.857 vs S_{ij} = 2.149). The final design has the solvent recovery at atmospheric conditions (P = 0.1013 MPa), and 99.51 wt % of both the components is achieved with P = 2.9 MPa, S/F = 8, and N_T = 50, but this high pressure resulted in a high Q_{Reb} and exceeded the operating temperature constraint with T_{Reb} = 473.5 K.

Overall, the azeotropic refrigerant mixtures can be separated to refrigerant purities of about 99.5 wt % using the proper IL entrainers. Future work should include rate-based models for sizing extractive distillation columns, heat exchangers, and pumps, as well as instrumentation logic. Additional properties will be required for rate-based models such as density, viscosity, surface tension, and liquid heat capacity for refrigerants and ILs. For the *PTx* systems that predict the LLE regions, the LLE data is also necessary for accurate modeling of refrigerant solubility over the entire composition range. Future work should investigate the interesting behavior for HFC-125 being more soluble in ILs containing the $[Ac]^-$ and $[Cl]^-$ anions.

■ ASSOCIATED CONTENT

Supporting Information

The Supporting Information is available free of charge at https://pubs.acs.org/doi/10.1021/acs.iecr.3c02180.

HFC/HFO refrigerant mixture compositions; IL chemical names; IL pseudo-critical properties and $\Delta C_{P,IG}$; *PTx* diagrams of experimental data compared to regression fit and *PTx* comparison diagrams (in both mole and mass fraction); summary of regression results for parameters k_{ij} and l_{ij} and the AAD of T, P, and x_i for each dataset; mass distilled vs distillate rate diagram of the equimass mixture HFC-32, HFC-125, HFC-134a, and HFO-1234yf; PFD of HFC-125/HFC-143a separation using $[P_{(14)666}][TMPP]$ with a vacuum flash vessel; PFD of HFC-125/HFC-143a separation using $[P_{(14)666}][TMPP]$ with a vacuum flash vessel and a higher S/F; and PFD of HFC-32/HCFC-22 separation using $[C_2C_1im][TFES]$ with a vacuum flash vessel (PDF)

■ AUTHOR INFORMATION

Corresponding Author

Mark B. Shiflett − *Institute for Sustainable Engineering, Lawrence, Kansas 66045, United States; Department of Chemical and Petroleum Engineering, University of Kansas, Lawrence, Kansas 66045, United States;* orcid.org/0000-0002-8934-6192; Email: mark.b.shiflett@ku.edu

Authors

Ethan A. Finberg − *Institute for Sustainable Engineering, Lawrence, Kansas 66045, United States; Department of Chemical and Petroleum Engineering, University of Kansas, Lawrence, Kansas 66045, United States;* orcid.org/0000-0002-4702-016X

Max Cordry − *Institute for Sustainable Engineering, Lawrence, Kansas 66045, United States; Department of Chemical and Petroleum Engineering, University of Kansas, Lawrence, Kansas 66045, United States*

Tessie L. May − *Institute for Sustainable Engineering, Lawrence, Kansas 66045, United States; Department of Chemical and Petroleum Engineering, University of Kansas,*

Lawrence, Kansas 66045, United States; orcid.org/0000-0002-3000-9765

Kalin R. Baca − *Institute for Sustainable Engineering, Lawrence, Kansas 66045, United States; Department of Chemical and Petroleum Engineering, University of Kansas, Lawrence, Kansas 66045, United States;* orcid.org/0000-0002-7292-8698

Complete contact information is available at: https://pubs.acs.org/10.1021/acs.iecr.3c02180

Notes

The authors declare no competing financial interest.

REFERENCES

(1) Article 2F: HydrochlorofluorocarbonsǀOzone Secretariat. https://ozone.unep.org/treaties/montreal-protocol/articles/article-2f-hydrochlorofluorocarbons (accessed 2022-10-02).

(2) Article 2A: CFCsǀOzone Secretariat. https://ozone.unep.org/treaties/montreal-protocol/articles/article-2a-cfcs (accessed 2022-10-02).

(3) The Kigali Amendment (2016): The amendment to the Montreal Protocol agreed by the Twenty-Eighth Meeting of the Parties (Kigali, 10-15 October 2016)ǀOzone Secretariat. https://ozone.unep.org/treaties/montreal-protocol/amendments/kigali-amendment-2016-amendment-montreal-protocol-agreed (accessed 2022-10-02).

(4) U.S.C. Title 42—the public health and welfare. https://www.govinfo.gov/content/pkg/USCODE-2013-title42/html/USCODE-2013-title42-chap85.htm (accessed 2022-10-22).

(5) Booten, C.; Nicholson, S.; Mann, M.; Abdelaziz, O. Refrigerants: Market Trends and Supply Chain Assessment; Golden. 2020. www.osti.gov/scitech (accessed 2022-10-02).

(6) Shiflett, M. B.; Maginn, E. J. The Solubility of Gases in Ionic Liquids. *AIChE J.* **2017**, *63*, 4722−4737.

(7) Lei, Z.; Dai, C.; Chen, B. Gas Solubility in Ionic Liquids. *Chem. Rev.* **2014**, *114*, 1289−1326.

(8) Mellein, B. R.; Scurto, A. M.; Shiflett, M. B. Gas Solubility in Ionic Liquids. *Curr. Opin. Green Sustainable Chem.* **2021**, *28*, 100425.

(9) Shiflett, M. B.; Yokozeki, A. Solubility and Diffusivity of Hydrofluorocarbons in Room-Temperature Ionic Liquids. *AIChE J.* **2006**, *52*, 1205−1219.

(10) Finberg, E. A.; May, T. L.; Shiflett, M. B. Multicomponent Refrigerant Separation Using Extractive Distillation with Ionic Liquids. *Ind. Eng. Chem. Res.* **2022**, *61*, 9795−9812.

(11) Finberg, E. A.; Shiflett, M. B. Process Designs for Separating R-410A, R-404A, and R-407C Using Extractive Distillation and Ionic Liquid Entrainers. *Ind. Eng. Chem. Res.* **2021**, *60*, 16054−16067.

(12) Monjur, M. S.; Iftakher, A.; Hasan, M. M. F. Separation Process Synthesis for High-GWP Refrigerant Mixtures: Extractive Distillation Using Ionic Liquids. *Ind. Eng. Chem. Res.* **2022**, *61*, 4390−4406.

(13) Asensio-Delgado, S.; Pardo, F.; Zarca, G.; Urtiaga, A. Absorption Separation of Fluorinated Refrigerant Gases with Ionic Liquids: Equilibrium, Mass Transport, and Process Design. *Sep. Purif. Technol.* **2021**, *276*, 119363.

(14) Kamiaka, T.; Dang, C.; Hihara, E. Vapor-Liquid Equilibrium Measurements for Binary Mixtures of R1234yf with R32, R125, and R134a. *Int. J. Refrig.* **2013**, *36*, 965−971.

(15) Hu, X.; Yang, T.; Meng, X.; Bi, S.; Wu, J. Vapor Liquid Equilibrium Measurements for Difluoromethane (R32) + 2,3,3,3-Tetrafluoroprop-1-Ene (R1234yf) and Fluoroethane (R161) + 2,3,3,3-Tetrafluoroprop-1-Ene (R1234yf). *Fluid Phase Equilib.* **2017**, *438*, 10−17.

(16) Peng, D. Y.; Robinson, D. B. A New Two-Constant Equation of State. *Ind. Eng. Chem. Fund.* **1976**, *15*, 59−64.

(17) Mathias, P. M.; Klotz, H. C.; Prausnitz, J. M. Equation-of-State Mixing Rules for Multicomponent Mixtures: The Problem of Invariance. *Fluid Phase Equilib.* **1991**, *67*, 31−44.

(18) Valderrama, J. O.; Robles, P. A. Critical Properties, Normal Boiling Temperatures, and Acentric Factors of Fifty Ionic Liquids. *Ind. Eng. Chem. Res.* **2007**, *46*, 1338−1344.

(19) Valderrama, J. O.; Rojas, R. E. Critical Properties of Ionic Liquids. Revisited. *Ind. Eng. Chem. Res.* **2009**, *48*, 6890−6900.

(20) Ge, R.; Hardacre, C.; Jacquemin, J.; Nancarrow, P.; Rooney, D. W. Heat Capacities of Ionic Liquids as a Function of Temperature at 0.1 MPa. Measurement and Prediction. *J. Chem. Eng. Data* **2008**, *53*, 2148−2153.

(21) Cam, L. L. Maximum Likelihood: An Introduction. *Int. Stat. Rev.* **1990**, *58*, 153.

(22) Liu, X.; He, M.; Lv, N.; Qi, X.; Su, C. Vapor-Liquid Equilibrium of Three Hydrofluorocarbons with [HMIM] [Tf2N]. *J. Chem. Eng. Data* **2015**, *60*, 1354−1361.

(23) Ren, W.; Scurto, A. M. Phase Equilibria of Imidazolium Ionic Liquids and the Refrigerant Gas, 1,1,1,2-Tetrafluoroethane (R-134a). *Fluid Phase Equilib.* **2009**, *286*, 1−7.

(24) Shiflett, M. B.; Yokozeki, A. Vapor-Liquid-Liquid Equilibria of Pentafluoroethane and Ionic Liquid [Bmim] [PF6] Mixtures Studied with the Volumetric Method. *J. Phys. Chem. B* **2006**, *110*, 14436−14443.

(25) Shiflett, M. B.; Yokozeki, A. Vapor - Liquid - Liquid Equilibria of Hydrofluorocarbons + 1-Butyl-3-Methylimidazolium Hexafluorophosphate. *J. Chem. Eng. Data* **2006**, *51*, 1931−1939.

(26) Ahosseini, A.; Ren, W.; Weatherley, L. R.; Scurto, A. M. Viscosity and Self-Diffusivity of Ionic Liquids with Compressed Hydrofluorocarbons: 1-Hexyl-3-Methyl-Imidazolium Bis-(Trifluoromethylsulfonyl)Amide and 1,1,1,2-Tetrafluoroethane. *Fluid Phase Equilib.* **2017**, *437*, 34−42.

(27) Morais, A. R. C.; Harders, A. N.; Baca, K. R.; Olsen, G. M.; Befort, B. J.; Dowling, A. W.; Maginn, E. J.; Shiflett, M. B. Phase Equilibria, Diffusivities, and Equation of State Modeling of HFC-32 and HFC-125 in Imidazolium-Based Ionic Liquids for the Separation of R-410A. *Ind. Eng. Chem. Res.* **2020**, *59*, 18222−18235.

(28) Zhang, Y.; Yin, J.; Wang, X. Vapor-Liquid Equilibrium of 2,3,3,3-Tetrafluoroprop-1-Ene with 1-Butyl-3-Methylimidazolium Hexafluorophosphate, 1-Hexyl-3-Methyl Imidazolium Hexafluorophosphate, and 1-Octyl-3-Methylimidazolium Hexafluorophosphate. *J. Mol. Liq.* **2018**, *260*, 203−208.

(29) Larriba, M.; García, S.; García, J.; Torrecilla, J. S.; Rodríguez, F. Thermophysical Properties of 1-Ethyl-3-Methylimidazolium 1,1,2,2-Tetrafluoroethanesulfonate and 1-Ethyl-3-Methylimidazolium Ethylsulfate Ionic Liquids as a Function of Temperature. *J. Chem. Eng. Data* **2011**, *56*, 3589−3597.

(30) Shiflett, M. B.; Harmer, M. A.; Junk, C. P.; Yokozeki, A. Solubility and Diffusivity of Difluoromethane in Room-Temperature Ionic Liquids. *J. Chem. Eng. Data* **2006**, *51*, 483−495.

(31) Sosa, J. E.; Ribeiro, R. P. P. L.; Castro, P. J.; Mota, J. P. B.; Araújo, J. M. M.; Pereiro, A. B. Absorption of Fluorinated Greenhouse Gases Using Fluorinated Ionic Liquids. *Ind. Eng. Chem. Res.* **2019**, *58*, 20769−20778.

(32) Minnick, D. L.; Shiflett, M. B. Solubility and Diffusivity of Chlorodifluoromethane in Imidazolium Ionic Liquids: [Emim] [Tf2N], [Bmim] [BF4], [Bmim] [PF6], and [Emim] [TFES]. *Ind. Eng. Chem. Res.* **2019**, *58*, 11072−11081.

(33) Blahušiak, M.; Schlosser, Š. Physical Properties of Phosphonium Ionic Liquid and Its Mixtures with Dodecane and Water. *J. Chem. Thermodyn.* **2014**, *72*, 54−64.

(34) Liu, X.; He, M.; Lv, N.; Qi, X.; Su, C. Solubilities of R-161 and R-143a in 1-Hexyl-3-Methylimidazolium Bis-(Trifluoromethylsulfonyl)Imide. *Fluid Phase Equilib.* **2015**, *388*, 37−42.

(35) Liu, X.; Qi, X.; Lv, N.; He, M. Gaseous Absorption of Fluorinated Ethanes by Ionic Liquids. *Fluid Phase Equilib.* **2015**, *405*, 1−6.

(36) Sun, Y.; Di, G.; Wang, J.; Hu, Y.; Wang, X.; He, M. Gaseous Solubility and Thermodynamic Performance of Absorption System Using R1234yf/IL Working Pairs. *Appl. Therm. Eng.* **2020**, *172*, 115161.

(37) Dong, L.; Zheng, D.; Sun, G.; Wu, X. Vapor-Liquid Equilibrium Measurements of Difluoromethane + [Emim]OTf, Difluoromethane + [Bmim]OTf, Difluoroethane + [Emim]OTf, and Difluoroethane + [Bmim]OTf Systems. *J. Chem. Eng. Data* **2011**, *56*, 3663−3668.
(38) Asensio-Delgado, S.; Pardo, F.; Zarca, G.; Urtiaga, A. Vapor-Liquid Equilibria and Diffusion Coefficients of Difluoromethane, 1,1,1,2-Tetrafluoroethane, and 2,3,3,3-Tetrafluoropropene in Low-Viscosity Ionic Liquids. *J. Chem. Eng. Data* **2020**, *65*, 4242−4251.
(39) Asensio-Delgado, S.; Pardo, F.; Zarca, G.; Urtiaga, A. Enhanced Absorption Separation of Hydrofluorocarbon/Hydrofluoroolefin Refrigerant Blends Using Ionic Liquids. *Sep. Purif. Technol.* **2020**, *249*, 117136.
(40) Asensio-Delgado, S.; Viar, M.; Pardo, F.; Zarca, G.; Urtiaga, A. Gas Solubility and Diffusivity of Hydrofluorocarbons and Hydrofluoroolefins in Cyanide-Based Ionic Liquids for the Separation of Refrigerant Mixtures. *Fluid Phase Equilib.* **2021**, *549*, 113210.
(41) Shiflett, M. B.; Yokozeki, A. Binary Vapor-Liquid and Vapor-Liquid-Liquid Equilibria of Hydrofluorocarbons (HFC-125 and HFC-143a) and Hydrofluoroethers (HFE-125 and HFE-143a) with Ionic Liquid [Emim] [Tf2N]. *J. Chem. Eng. Data* **2008**, *53*, 492−497.
(42) Ren, W.; Scurto, A. M.; Shiflett, M. B.; Yokozeki, A. Phase Behavior and Equilibria of Ionic Liquids and Refrigerants: 1-Ethyl-3-Methyl-Imidazolium Bis(Trifluoromethylsulfonyl)Imide ([EMIm][Tf 2N]) and R-134a. ACS Symposium Series; American Chemical Society, 2009; Vol. *1006*, pp 112−128.
(43) Lepre, L. F.; Andre, D.; Denis-Quanquin, S.; Gautier, A.; Pádua, A. A. H.; Costa Gomes, M. Ionic Liquids Can Enable the Recycling of Fluorinated Greenhouse Gases. *ACS Sustain. Chem. Eng.* **2019**, *7*, 16900−16906.
(44) Shiflett, M. B.; Yokozeki, A. Solubility Differences of Halocarbon Isomers in Ionic Liquid [Emim] [Tf2N]. *J. Chem. Eng. Data* **2007**, *52*, 2007−2015.
(45) Liu, X.; Bai, L.; Liu, S.; He, M. Vapor−liquid Equilibrium of R1234yf/[HMIM] [Tf2N] and R1234ze(E)/[HMIM] [Tf2N] Working Pairs for the Absorption Refrigeration Cycle. *J. Chem. Eng. Data* **2016**, *61*, 3952−3957.
(46) Baca, K. R.; Olsen, G. M.; Matamoros Valenciano, L.; Bennett, M. G.; Haggard, D. M.; Befort, B. J.; Garciadiego, A.; Dowling, A. W.; Maginn, E. J.; Shiflett, M. B. Phase Equilibria and Diffusivities of HFC-32 and HFC-125 in Ionic Liquids for the Separation of R-410A. *ACS Sustain. Chem. Eng.* **2022**, *10*, 816−830.
(47) Freire, M. G.; Teles, A. R. R.; Rocha, M. A. A.; Schröder, B.; Neves, C. M. S. S.; Carvalho, P. J.; Evtuguin, D. V.; Santos, L. M. N. B. F.; Coutinho, J. A. P. Thermophysical Characterization of Ionic Liquids Able To Dissolve Biomass. *J. Chem. Eng. Data* **2011**, *56*, 4813−4822.
(48) Williams, M. L.; Holahan, S. P.; McCorkill, M. E.; Dickmann, J. S.; Kiran, E. Thermal and Spectral Characterization and Stability of Mixtures of Ionic Liquids [EMIM]Ac and [BMIM]Ac with Ethanol, Methanol, and Water at Ambient Conditions and at Elevated Temperatures and Pressures. *Thermochim. Acta* **2018**, *669*, 126−139.
(49) Muldoon, M. J.; Aki, S. N. V. K.; Anderson, J. L.; Dixon, J. K.; Brennecke, J. F. Improving Carbon Dioxide Solubility in Ionic Liquids. *J. Phys. Chem. B* **2007**, *111*, 9001−9009.
(50) Shiflett, M. B.; Yokozeki, A. Phase Behavior of Carbon Dioxide in Ionic Liquids: [Emim] [Acetate], [Emim] [Trifluoroacetate], and [Emim] [Acetate] + [Emim] [Trifluoroacetate] Mixtures. *J. Chem. Eng. Data* **2009**, *54*, 108−114.
(51) Shiflett, M. B.; Drew, D. W.; Cantini, R. A.; Yokozeki, A. Carbon Dioxide Capture Using Ionic Liquid 1-Butyl-3-Methylimidazolium Acetate. *Energy Fuel.* **2010**, *24*, 5781−5789.
(52) Maginn, E. J. *Design and Evaluation of Ionic Liquids as Novel CO2 Absorbents*; Quarterly Technical Report to Department of Energy (DOE), 2006.

https://doi.org/10.1021/acs.iecr.3c02180
Ind. Eng. Chem. Res. 2023, 62, 16070−16080